THE JOURNAL OF BIOLOGICAL CHEMISTRY
Vol. 275, No. 43, Issue of October 27, pp. 33244–33251, 2000
Printed in U.S.A.

Characterization of the *Saccharomyces cerevisiae* High Affinity Copper Transporter Ctr3*

Received for publication, June 20, 2000, and in revised form, July 24, 2000
Published, JBC Papers in Press, August 2, 2000, DOI 10.1074/jbc.M005392200

Maria Marjorette O. Peña‡, Sergi Puig§, and Dennis J. Thiele¶

From the Department of Biological Chemistry, University of Michigan Medical School, Ann Arbor, Michigan 48109-0606

Copper is an essential nutrient required for the activity of a number of enzymes with diverse biological roles. In the bakers' yeast *Saccharomyces cerevisiae*, copper is transported into cells by two high affinity copper transport proteins, Ctr1 and Ctr3. Although Ctr1 and Ctr3 are functionally redundant, they bear little homology at the amino acid sequence level. In this report, we characterize Ctr3 with respect to its localization, assembly, and post-transcriptional regulation. Ctr3 is an integral membrane protein that assembles as a trimer to form a competent copper uptake permease at the plasma membrane. Whereas the *CTR1* and *CTR3* genes are similarly regulated at the transcriptional level in response to copper, post-transcriptional regulation of these proteins is distinct. Unlike Ctr1, the Ctr3 transporter is neither regulated at the level of protein degradation nor endocytosis as a function of elevated copper levels. Our studies suggest that Ctr3 constitutes a fundamental module found in all eukaryotic high affinity copper transporters to date, which is sufficient for copper uptake but lacks elements for post-transcriptional regulation by copper.

Copper is an essential redox active metal that serves as a cofactor in a variety of enzymes such as cytochrome oxidase, Cu,Zn superoxide dismutase, ceruloplasmin, and lysyl oxidase (1). When allowed to accumulate in excess, copper is toxic due to its proclivity to participate in Fenton-like reactions that lead to the generation of highly reactive hydroxyl radicals (2). Consequently, organisms have developed sophisticated mechanisms for maintaining the balance between essential and toxic copper levels. Studies of copper uptake in *Saccharomyces cerevisiae* have shown that copper is reduced from Cu(II) to Cu(I) by cell surface metalloreductases (3, 4) and transported by two high affinity copper transport proteins, Ctr1 and Ctr3 (5, 6). Within cells copper is distributed to specific subcellular compartments or proteins by copper chaperones that include Atx1 which delivers copper to the Fet3 high affinity iron transport subunit in the secretory compartment (7, 8), Cox17, which is required for delivery to mitochondrial cytochrome oxidase (9), and CCS, which inserts copper into Cu,Zn superoxide dismutase (10). Although inactivation of the yeast copper chaperone genes generates phenotypes specific for each copper delivery pathway, mutations in the both the *CTR1* and *CTR3* genes result in yeast cells that exhibit phenotypic defects associated with mutations in all three of the copper chaperone genes (5, 6). In addition, these cells are defective in high affinity copper uptake resulting in poor growth on low copper media and defective in their ability to activate transcription of the *CUP1*-encoded metallothionein, except at copper concentrations beyond the high affinity range, due to an inability to provide copper to the metalloregulatory transcription factor Ace1 (5, 6).

Because copper uptake at the cell membrane is a crucial step in copper acquisition, yeast genes encoding the high affinity copper transport proteins are tightly regulated in response to copper levels to ensure that sufficient copper is present for cellular needs. In *S. cerevisiae* transcription of the *CTR1* and *CTR3* genes is activated during copper starvation and repressed under conditions of copper adequacy (11–13). At the post-transcriptional level Ctr1 protein has been shown to be regulated by two distinct processes (14). At low copper concentrations (0.1–1 μM) Ctr1 undergoes copper-induced endocytosis, although the role of Ctr1 internalization in copper uptake is currently unclear. Furthermore, exposure of yeast cells to high copper concentrations ($\geq$10 μM) triggers the degradation of Ctr1 at the plasma membrane in a mechanism that is independent of endocytosis and vacuolar proteases (14).

The Ctr1 and Ctr3 high affinity copper transport proteins are functionally redundant. However, there is little homology between their amino acid sequences, and they are structurally distinct (15). Although both proteins possess three potential membrane spanning domains, Ctr1 is a 406-amino acid protein that is highly glycosylated and harbors eight repeats of the potential metal-binding motif MX_2MXM (Mets domain) in the predicted amino-terminal extracellular domain (5). These motifs are repeated twice in the putative human and mouse copper transport proteins, hCtr1 and mCtr1, and five times in the fission yeast *Schizosaccharomyces pombe* copper transport protein Ctr4 (15). Ctr3 lacks this motif but has an abundance of cysteine residues throughout the protein (11 Cys of 241 total residues) and within its putative transmembrane domains. Since both methionine and cysteine are potential copper-binding ligands (16), these residues may be important for copper uptake. Alignment of the sequences of Ctr1 and Ctr3 with the *S. pombe* Ctr4, human and mouse Ctr1, and putative copper transport proteins in existing data bases from *Caenorhabditis elegans* and *Drosophila melanogaster* reveal the following observations. First, the copper transport family of proteins is defined by the presence of three transmembrane domains. Second, with the exception of *S. cerevisiae* Ctr1, the transmembrane spanning regions exhibit high similarity to the Ctr3 transmembrane domains with several highly conserved residues present in all sequences. Third, the predicted ectodomains of the known copper transporters, and some of the putative copper transporters, are similar to Ctr1 with respect to the

---

* This work was supported in part by Grant GM41840 from the National Institutes of Health (to D. J. T.). The costs of publication of this article were defrayed in part by the payment of page charges. This article must therefore be hereby marked "*advertisement*" in accordance with 18 U.S.C. Section 1734 solely to indicate this fact.

‡ Recipient of Postdoctoral Fellowship 5F32GM18089 from the National Institutes of Health.

§ Recipient of a postdoctoral fellowship from the North Atlantic Treaty Organization.

¶ To whom correspondence should be addressed. Tel.: 734-763-5717; Fax: 734-763-4581; E-mail: dthiele@umich.edu.

TABLE I
Yeast strains used in this study

Strain	Genotype	Ref.
MPY17	*MATa ctr1::ura3::Kan*^{r} *ctr3::TRP1 his3 lys2-802 CUP1*^{r}	44
SKY52	*MATa gal1 trp1-1 his3 ade8 CUP1*^{r} *ctr1::TRP1*	6
RH1800	*MATa leu2 his4 ura3 bar1(wt)*	25
RH3777	*MATa ura3 leu2 his4 bar1 ts end3-1*	25
W303	*MATa SUC2 ade2-1 can1-100 his3-11,15 leu2-3,-112 trp1-1 ura3-1*	
KRY54-4	*MATα sec12-4 ura3-1 his3-11,-15 leu2-3,-112*	R. Fuller

presence of the MX$_2$MXM motif that is predicted to bind copper. The conservation of these domains between yeast and mammalian systems suggests an important functional role in copper binding and transport. Taken together, it appears possible that the fusion of *S. cerevisiae* Ctr1 and Ctr3-like proteins may be an early event that led to the evolution of high affinity copper transport proteins of other eukaryotes (15, 17).

Since most eukaryotic high affinity copper transporters identified to date have strong homology to Ctr3, it is important to understand the structure, function, and regulation of this protein. Here we show that Ctr3 exists as a trimer at the plasma membrane to form the competent copper uptake permease. Of the 11 cysteine residues distributed throughout Ctr3, only mutations in four of these amino acid residues affect Ctr3 function and localization. These mutants can assemble as a trimer, as assessed by *in vitro* cross-linking experiments; however, the mutant protein complexes fail to localize at the plasma membrane suggesting that assembly of the competent permease takes place in the secretory pathway. At the post-transcriptional level, Ctr3 is distinctly regulated compared with Ctr1 in response to copper.

EXPERIMENTAL PROCEDURES

Yeast Strains and Growth Conditions—The yeast strains used in this study are listed in Table I. Strains were maintained in YPD medium (1% yeast extract, 2% BactoPeptone, 2% dextrose) or in the corresponding drop-out media for the maintenance of yeast strains transformed with plasmids.

Plasmids—The plasmids pRS316-*CTR3* and pRS316-*CTR3-Not*I carry the *CTR3* open reading frame on a centromeric plasmid, with or without a *Not*I restriction site before the stop codon, respectively, and the *CTR3* promoter region up to −349 from the start codon for translation and the 3′ region up to +328 from the stop codon, cloned into the *Xho*I and *Sst*I sites. The plasmids pRS426-*CTR3* and pRS426-*CTR3-Not*I have the same *CTR3* fragments on a 2 μM plasmid. pRS416-*CTR3-GFP* and pRS426-*CTR3-GFP* were constructed by inserting a *Not*I fragment containing the green fluorescent protein (GFP)[1] (18) derived from pSF1-GP1 at the *Not*I sites of pRS416-*CTR3-NOTI* and pRS426-*CTR3-NOTI*. Construction of pRS416-*CTR3-FLAG*(*2*) was carried out as follows: two oligonucleotides, FLAG(2)UP (5′-GGCCGAGACTACAAGGACGACGATGACAAAGGCGACTACAAGGACGACGATGACAAAGAC-3′) and FLAG(2)LOW (5′-GGCCGTCTTTGTCATCGTCGTCCTTGTAGTCGCCTTTGTCATCGTCGTCCTTGTAGTCTC-3′), encoding two copies of the FLAG epitope (19), were boiled and annealed in the presence of 50 mM NaCl and 1× BRL ligation buffer generating *Eag*I overhangs. These oligonucleotides were ligated into *Not*I-digested pRS416-*CTR3-Not*I and pRS426-*CTR3-Not*I plasmids and digested with *Not*I prior to transformation into *Escherichia coli* DH5α′ cells. Proper orientation of the FLAG(2) tag was verified by dideoxy DNA sequencing. The plasmid pRS413-*CTR3-myc*(*2*) was constructed as described above using the following oligonucleotides: MYC(2)UP (5′-GGCCGAGAACAAAAGCTTATTTCTGAAGAAGACTTAGGCGAACAAAAGCTTATTTCTGAAGAAGACTTAGAC-3′) and MYC(2)DOWN (5′-GGCCGTCTAAGTCTTCTTCAGAAATAAGCTTTTGTTCGCCTAAGTCTTCTTCAGAAATAAGCTTTTGTTCTC-3′), encoding two copies of the c-*myc* epitope (20). To test whether insertion of the epitope tags and GFP interfered with Ctr3 function, the tagged *CTR3* genes were transformed into MPY17, a *ctr1*Δ *ctr3*Δ double deletion strain, and serial dilutions of the transformants tested for their ability to grow in ethanol, a non-fermentable carbon source.

Plasmids pRS423-GAL1-*CTR3-myc*(*2*) and pRS423-GAL1-*CTR3-FLAG*(*2*) were constructed as follows: two polymerase chain reaction fragments encompassing the *CTR3* open reading frame starting at −50 from the translational start codon up to +21 after the stop codon, including the epitope tags, were amplified using *Pfu* Turbo polymerase (Stratagene) from pRS413-*CTR3-myc*(*2*) and pRS416-*CTR3-FLAG*(*2*), respectively with the primers CTR3-START (5′-CGAAGAAGAGGGATACAACAG-3′) and CTR3-END (5′-CAAACCTCTCGGCTTTCCTCT-3′). These fragments were then cloned into the *Eco*RI and *Xho*I sites of pRS423-GAL1 (21). Plasmid p426-GAL1-*CTR1-GFP* was constructed by amplifying the *CTR1* open reading frame from genomic DNA using *Pfu* Turbo polymerase and the primers CTR1atgS (5′-GGACCCGGGATGGAAGGTATGAATATGGGT-3′) and CTR1tNPH (5′-CGGCTTTTTAAGTGAGTATTGCCGCCGGCGATTGACGTCTTCGAACCC-3′). The polymerase chain reaction fragment was cloned into the *Sma*I and *Hin*dIII sites on p426-Gal1 (21) and the GFP tag inserted into a *Not*I site engineered prior to the *CTR1* STOP codon.

Fluorescence Microscopy—For localization of Ctr3, MPY17 cells transformed with plasmids harboring the *CTR3-GFP* fusion were grown on YPE medium (1% yeast extract, 2% BactoPeptone, 3% ethanol). Cells were resuspended in liquid YPE and immobilized on slides with 1% low melting agarose. Ctr3-GFP was visualized by fluorescence microscopy using a Zeiss Axioskop photomicroscope with filters for observing green fluorescence. Cells were photographed with Kodak TMAX 400 print film. The negatives were digitized to CD-ROM and optimized for contrast and sharpness using Adobe Photoshop 3.0. For copper-dependent endocytosis of Ctr1 and Ctr3, fluorescence microscopy was carried out using a Nikon Eclipse E800 fluorescent microscope equipped with a Hamamatsu ORCA-2 cooled CCD camera. Images were obtained using ESee and ISee software packages from Innovision, Corp. (Raleigh-Durham, NC) and processed using Adobe Photoshop 3.0.

Biochemical Methods—For co-immunoprecipitation experiments, MPY17 cells were co-transformed with pRS416-*CTR3-FLAG*(*2*) *and* pRS413-*CTR3-myc*(*2*). Cells were grown to OD$_{650}$ = 1.0 in the presence of 10 μM of the copper chelator bathocuproine disulfonate (BCS). Total cell lysates were obtained by glass bead disruption in lysis buffer (25 mM Tris-HCl, pH 7.5, 150 mM NaCl) with protease inhibitors (10 μg/ml leupeptin, 20 μg/ml pepstatin, 10 μg/ml aprotinin, 2 mM phenylmethylsulfonyl fluoride, 0.5 mM 4-(2-aminoethyl)-benzenesulfonyl fluoride, and 1 tablet of Complete Mini EDTA-free protease inhibitor (Roche Molecular Biochemicals) per 10 ml of lysis buffer) followed by solubilization with 1% Triton X-100 on ice for 30 min and centrifugation at 15,000 × *g* at 4 °C for 15 min. Protein extracts were quantitated using bicinchoninic acid (Pierce). Co-immunoprecipitation of Ctr3-FLAG(2) and Ctr3-myc(2) was carried out on Triton X-100 extracts using anti-FLAG M2 Affi-Gel (Sigma) or anti-*c-myc* 9E10 (Roche Molecular Biochemicals) antibody as described previously (11). The immunoprecipitates were resuspended in Laemmli buffer and heated at 37 °C for 5 min prior to SDS-polyacrylamide gel electrophoresis and immunoblot analysis using standard protocols (22).

For *in vitro* cross-linking experiments, total cell lysate was prepared from cells expressing Ctr3-FLAG(2) as described above using phosphate-buffered saline (PBS) instead of Tris-HCl. Lysates were incubated for 30 min at room temperature with increasing concentrations of ethylene glycol bis(succinimidylsuccinate) (EGS) (Pierce) using stock solutions of 15 and 50 mM EGS in dimethyl sulfoxide (Me$_2$SO). The cross-linking reaction was quenched with 45 mM Tris-HCl, pH 7.5, followed by incubation for 30 min at room temperature. The cross-linked products were analyzed by SDS-PAGE and immunoblotting. Cross-linking experiments using EGS were also carried out on intact membranes obtained from lysed spheroplasts as described previously (23, 24) with the following modifications. The membranes were washed

---

[1] The abbreviations used are: GFP, green fluorescent protein; PAGE, polyacrylamide gel electrophoresis; ER, endoplasmic reticulum; EGS, ethylene glycol bis(succinimidylsuccinate); BCS, bathocuproine disulfonic acid; PBS, phosphate-buffered saline; PAGE, polyacrylamide gel electrophoresis.

with PBS prior to cross-linking. After cross-linking, the membranes were incubated with 1% Triton X-100 for 30 min on ice to solubilize the membranes followed by centrifugation at 15,000 rpm for 15 min at 4 °C. The cross-linked complexes were immunoprecipitated from the clarified extracts using anti-FLAG M2 Affi-Gel beads for 1 h at 4 °C in the presence of fresh protease inhibitors. The beads were washed three times with lysis buffer containing 1% Triton X-100, and the complexes were eluted from the beads with 0.1 M glycine, pH 3.0 and neutralized with 1.0 M Tris-HCl, pH 8.0. The immunoprecipitated complexes were analyzed by SDS-PAGE under denaturing and non-denaturing conditions and immunoblotting.

Degradation and Endocytosis Experiments—For the analysis of copper-induced degradation of Ctr3 and Ctr1, W303 cells were transformed with p426-Gal1-*CTR3-FLAG(2)* and p426-Gal1-*CTR1-myc*. For copper-dependent endocytosis wild type (RH1800) cells and the corresponding endocytosis-deficient mutant, RH3777 (*end3–1*) (25), were transformed with p426-Gal1-*CTR3-GFP* and p426-Gal1-*CTR1-GFP*. Cells were grown and treated with copper or BCS as described previously (14). For endocytosis experiments, cells were incubated at 15 °C for 15 min while shaking at 300 rpm, followed by the addition of 10 μM copper sulfate or BCS. After 1 h incubation, cells were treated with one-tenth volume of KILL buffer (1.0 M Tris-HCl, pH 7.5, 100 mM sodium azide, 100 mM sodium fluoride) to stop endocytosis (26). Endocytosis of Ctr3-GFP and Ctr1-GFP was observed using a Nikon microscope as described above.

Site-directed Mutagenesis—Site-directed mutagenesis of the *CTR3* gene was performed using the Chameleon^{TM} Double-stranded Site-directed Mutagenesis Kit (Stratagene) following the manufacturer's instructions. Specific oligonucleotides were synthesized to convert cysteine residues to serine or alanine and tyrosine residues to phenylalanine. The template used for mutagenesis was pIBI30-*CTR3* containing the *CTR3* open reading frame with 349 base pairs of the 5′ promoter and 328 base pairs of the 3′-flanking regions. The mutated genes were cloned into pRS316 at the *Xho*I and *Sst*I sites and transformed into *S. cerevisiae* MPY17 cells to test for function.

RESULTS

Localization of the Ctr3 Protein—Our previous localization studies of Ctr3, using a Ctr3-HA-tagged allele, found that it predominantly localized to intracellular vesicles consistent with the secretory compartment (6). However, subsequent phenotypic analysis of the Ctr3-HA epitope-tagged protein demonstrated that it is only partially functional in high affinity copper transport. To facilitate a re-analysis of the localization and biochemical characterization of Ctr3, a plasmid-borne copy of *CTR3* was engineered to add a *Not*I site at the carboxyl terminus just prior to the STOP codon for the insertion of different epitopes. Two copies each of the FLAG epitope, c-*myc* epitope, and a single copy of the GFP were inserted into the *Not*I site. Plasmids expressing the tagged Ctr3 proteins were transformed into a *ctr1*Δ *ctr3*Δ strain, and a serial dilution series of each culture was analyzed for respiratory competency as compared with the wild type *CTR3* gene. As shown in Fig. 1*A*, all of the epitope-tagged alleles used in this study functionally complement the respiratory deficiency of a *ctr1*Δ *ctr3*Δ strain in a manner indistinguishable from the *CTR3* wild type allele.

The Ctr3-GFP fusion protein was localized to the plasma membrane by fluorescence microscopy (Fig. 1*B*). As a control, a functional fusion between the yeast heat shock transcription factor and GFP was localized to the nucleus (27), and the unfused GFP protein was distributed throughout cells. To ascertain if Ctr3 traverses the normal route for plasma membrane proteins through the secretory pathway for localization to the plasma membrane, Ctr3-GFP was expressed and localized in temperature-sensitive *sec12-4* mutant cells. Although at the permissive temperature protein secretion is normal in the *sec12-4* background, at the non-permissive temperature (37 °C) transport from the ER to the Golgi is blocked in this mutant (28, 29). The *sec12-4* mutant cells expressing Ctr3-GFP were grown at the permissive (25 °C) and non-permissive temperatures, and Ctr3-GFP protein was localized by fluorescence microscopy. At the permissive temperature in both wild type and *sec12-4* cells Ctr3-GFP was localized to the plasma membrane. However, at the restrictive temperature in *sec12-4* cells, but not wild type cells, Ctr3-GFP was trapped in a perinuclear compartment that is likely to be the ER (Fig. 1*C*). This was observed for the Ctr3-GFP fusion protein expressed from either a single copy plasmid or a high copy plasmid where ER extensions approaching the plasma membrane are visible. These experiments demonstrate that, consistent with its role in copper uptake, the normal localization of Ctr3 is at the plasma membrane.

Multimerization of Ctr3—The primary sequences of the known or predicted high affinity copper transport proteins in yeast, mouse, and human all predict the presence of three membrane spanning domains. This feature is unique in that the numerous membrane permeases and transport proteins that have been characterized in yeast possess at least 6 and up to 12 or more transmembrane domains (30). Furthermore, metal ion transporters that have been characterized in both yeast and mammalian cells that transport zinc, iron, intracellular copper, and other metals have at least 6 and up to 12 transmembrane domains (31). Because several membrane spanning domains are thought to be important for the formation of a membrane channel, we examined the possibility that Ctr3 multimerizes to form the competent copper-transporting permease. Ctr3-FLAG(2) and Ctr3-myc(2) were co-expressed from different plasmids in a *ctr1*Δ *ctr3*Δ double deletion strain. Total Triton X-100-solubilized extracts from these cells were immunoprecipitated with anti-FLAG M2 antibody, immunoprecipitates resolved by SDS-PAGE, and analyzed by immunoblotting using anti-*c-myc* 9E10 antibody. The converse experiment was performed by immunoprecipitation with the anti-*c-myc* 9E10 antibody and immunoblot analysis using anti-FLAG M2 antibody. As shown in Fig. 2, Ctr3-myc(2) and Ctr3-FLAG(2) can be detected in total protein extracts from cells expressing either protein by itself (Fig. 2, *lanes 2* and *3*) or with the other protein (Fig. 2, *lane 4*). However, immunoprecipitation of Ctr3-myc(2) with anti-FLAG M2 antibody can be accomplished only when it is co-expressed with Ctr3-FLAG(2) (Fig. 2, *lane 8*). Conversely, Ctr3-FLAG(2) can be immunoprecipitated with anti-*c-myc* 9E10 antibody only when it is co-expressed with Ctr3-myc(2) (Fig. 2, *lane 8*), suggesting that these differentially tagged Ctr3 molecules can assemble into a multimeric complex when co-expressed in the same cells. Neither protein can be detected in cells that were transformed with vectors only (Fig. 2, *lane 1*). To assess the specificity of the co-immunoprecipitations, the total cell lysates and immunoprecipitates were probed with polyclonal antibodies against Pma1, the plasma membrane H^+ATPase that is detected as a 100-kDa protein (32), and Gas1, a glycophosphatidylinositol-anchored membrane glycoprotein (33). Two forms of Gas1 are detected, the 125-kDa plasma membrane-bound protein and the 113-kDa ER form of the protein (33). As shown in Fig. 2, both Pma1 and Gas1 are present in the total cell extracts (*lanes 1–4*) but not in the immunoprecipitates. These observations suggest that the Ctr3-FLAG(2) and Ctr3-myc(2) proteins specifically associate with each other to form a stable mixed multimer that can be co-immunoprecipitated from cell extracts. A similar observation has been reported for the *S. cerevisiae* Ctr1 protein (11).

To estimate the stoichiometry of Ctr3 molecules present in a copper transport complex, cross-linking experiments were carried out on Triton X-100-solubilized total cell extracts from cells expressing Ctr3-FLAG(2) using the cross-linking agent EGS (34). The cross-linked products were resolved by SDS-PAGE and analyzed by immunoblotting using anti-FLAG M2 antibody. In the absence of EGS, Ctr3-FLAG(2) migrates as a 27-kDa monomeric protein (Fig. 3*A, lane 1*) consistent with its predicted mass and suggesting little or no glycosylation. As the

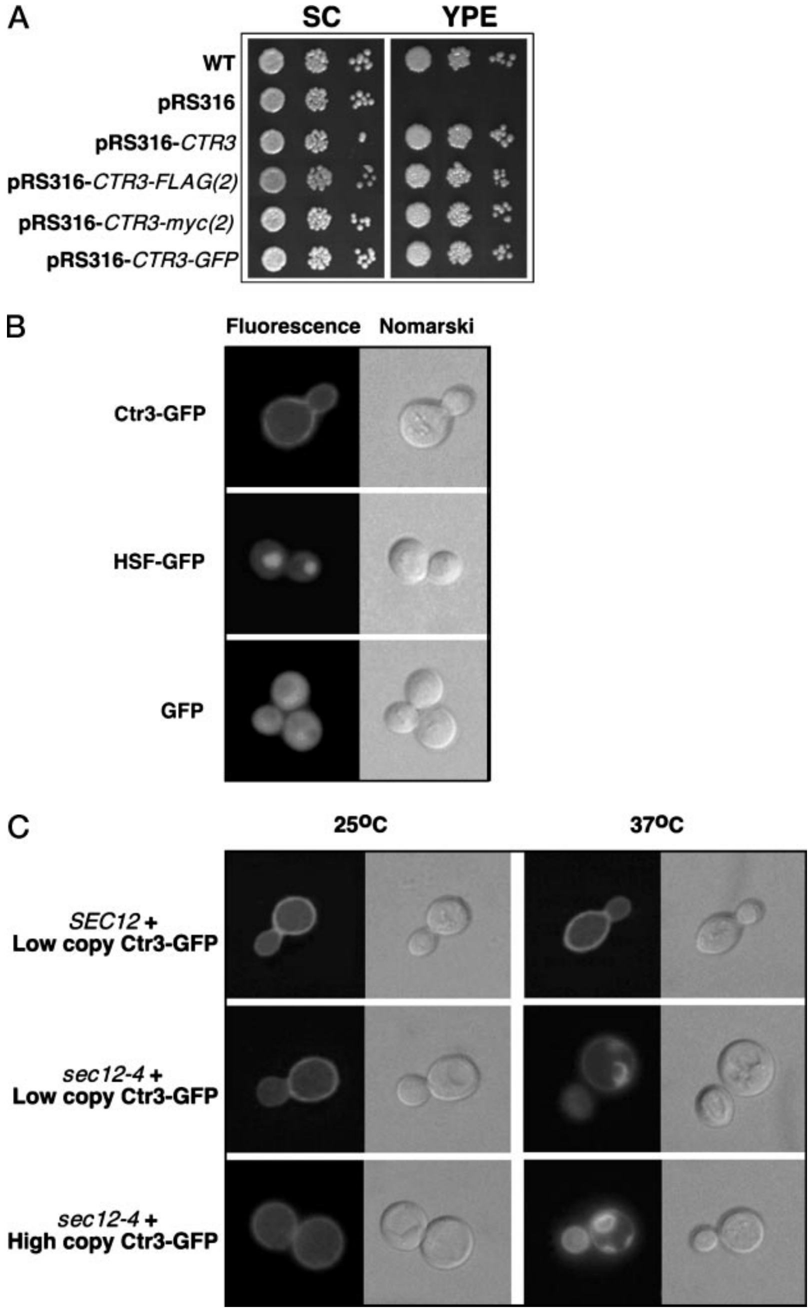

FIG. 1. **Ctr3 is localized to the plasma membrane.** *A*, tagged Ctr3 proteins are functional. Yeast cells (MPY17) harboring a *ctr1*Δ *ctr3*Δ double deletion were transformed with the pRS316 plasmid carrying the *CTR3* gene encoding Ctr3 fused to two copies of the FLAG or c-*myc* epitope at the carboxyl terminus and under the control of the *CTR3* promoter, pRS316-*CTR3-FLAG*(*2*) and pRS316-*CTR3-MYC*(*2*), respectively, a carboxyl-terminal fusion of CTR3 to the green fluorescent protein, pRS316-*CTR3-GFP*, wild type (*WT*) copy of *CTR3*, pRS316-*CTR3*, and vector only, pRS316. Three 10-fold serial dilutions (*left* to *right*) of the transformed cells were plated on non-selective media, SC, and on media containing 2% ethanol as a carbon source, YPE, to test the ability of the epitope-tagged Ctr3 proteins to complement the respiratory defect of MPY17 cells. In this medium, copper transport is required to provide copper to cytochrome oxidase to allow growth by respiration. Growth rates of the transformed cells were compared with a strain containing a genomic copy of CTR3, WT. Cells were grown for 3 days at 30 °C and photographed. *B*, localization of Ctr3 at the plasma membrane. MPY17 cells were transformed with pRS416-*CTR3-GFP* and grown in media containing ethanol. These cells were also transformed with p413-GPD-*HSF-GFP* and p413-GPD-*GFP* as a control for nuclear and cytoplasmic localization, respectively. Fluorescence microscopy was used to visualize the cellular location of GFP fusions and GFP alone, and cell morphology was examined using Nomarski optics. *HSF-GFP,* heat shock transcription factor and GFP. *C*, KRY54-4 cells harboring a *sec12-4* temperature-sensitive mutation and the corresponding parental wild type strain were transformed with pRS416-*CTR3-GFP* and pRS426-*CTR3-GFP*. Cells were grown in the presence of BCS at the permissive temperature of 25 °C or the restrictive temperature of 37 °C in which the *sec12-4* mutants are blocked in protein transport from the ER to the Golgi. The GFP fusion proteins were visualized by fluorescence microscopy, and cell morphology was viewed though Nomarski optics. Shown are representative cells from cultures of similar cells.

EGS concentration is increased, Ctr3-FLAG(2) forms a ~54-kDa complex consistent with the size expected for a Ctr3 homodimer (Fig. 3*A, lane 2*), and at 0.5 mM EGS an ~82-kDa complex, equivalent to the size expected for a Ctr3 homotrimer, is detected (Fig. 3*A, lane 3*). As the EGS concentration is increased to 1.0 mM, the dimeric and trimeric forms are detected with concomitant disappearance of the 27-kDa monomeric Ctr3-FLAG(2) (*lane 4*). In the presence of 2 and 3 mM EGS, the monomeric and dimeric forms are completely chased into a trimer with no observed formation of additional higher molecular weight complexes at this or higher EGS concentrations (Fig. 3*A, lanes 5* and *6*).

To test whether Ctr3 exists as a trimer at the plasma membrane, cross-linking reactions were performed on intact plasma membranes obtained from lysed spheroplasts made from cells expressing Ctr3-FLAG(2), as well as untransformed MPY17 cells as a negative control. The EGS-cross-linked complexes were extracted from the plasma membrane as described under "Experimental Procedures." The immunoprecipitates were resuspended in non-denaturing buffer (no β-mercaptoethanol or SDS and 0.01 M iodoacetamide to prevent the rearrangement of disulfide bonds) or denaturing sample buffer (5% β-mercaptoethanol and 2% SDS) (22) and analyzed by immunoblotting using anti-FLAG M2 antibody. As shown in Fig. 3*B*, under native conditions, in the absence of EGS, high molecular weight species migrating at ~75-kDa and higher are detected (*lane 1*), which dissociate into the 27-kDa monomeric and ~54-kDa dimeric forms under denaturing conditions (*lane 5*). As the EGS concentration increases, high molecular weight species that may correspond to homotrimers are detected under native conditions (*lanes 2–4*). Under denaturing conditions, in the presence of 1 and 2 mM EGS, the high molecular weight species are resistant to denaturation and migrate as a mixture of dimers and trimers (*lanes 6* and *7*). In the presence of 3 mM EGS, these species exist primarily as a trimer under both native and denaturing conditions (*lanes 4* and *8*). Under native conditions, the mobility of the high molecular weight complexes do not correspond to their predicted molecular weights (*lanes*

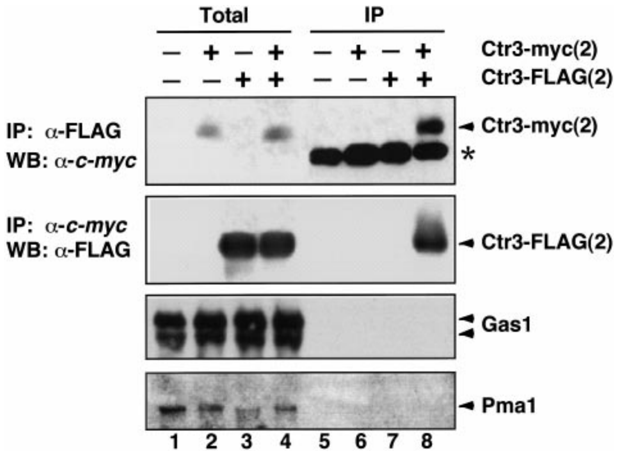

FIG. 2. **Multimerization of Ctr3.** Strain MPY17 (*ctr1*Δ *ctr3*Δ) was transformed with FLAG-tagged (pRS316-*CTR3-FLAG*(*2*)) (*lane 2*) or Myc-tagged (pRS413-*CTR3-Myc*(*2*)) (*lane 3*) Ctr3 individually or with both plasmids (*lane 4*). As a control, these cells were also transformed with pRS316 and pRS413 vectors (*lane 1*). The transformants were grown to log phase and treated with 10 μM BCS for 3 h to induce expression of Ctr3. Triton X-100-solubilized extracts were used for immunoprecipitation and the immunoprecipitates (*IP*) (*lanes 5–8*) as well as total extracts (*Total*) (*lanes 1–4*) were separated on 12% SDS-PAGE gels and visualized by immunoblotting (WB). Extracts were immunoprecipitated with anti-FLAG M2 Affi-Gel and visualized with anti-c-*myc* antibody or immunoprecipitated with anti-c-*myc* antibody and visualized with anti-FLAG M2 antibody. Ctr3-FLAG(2) and Ctr3-myc(2) are indicated by *labeled arrows.* As a specificity control, blots were stripped and probed with anti-Gas1 antibody and anti-Pma1 antibody which are indicated by *labeled arrows.* The *asterisk* represents the position of the light chain from the immunoprecipitating antibody.

1–4) possibly due to aberrant migration during electrophoresis under these conditions. No complexes were detected in untransformed *ctr1*Δ *ctr3*Δ cells (data not shown). These results suggest that indeed Ctr3 can be isolated as a pre-formed trimer from plasma membrane preparations. This homotrimer may represent the functional copper transport complex at the plasma membrane.

Importance of Cysteine Residues for Ctr3 Function—The biochemical mechanisms by which copper transport proteins mediate the uptake of copper into cells is poorly understood. The presence of the potential metal-binding motif, MX_2MXM, within the amino-terminal ectodomain of Ctr1 from yeast and mammals suggests that these motifs may be involved in binding copper ions from the extracellular milieu for transport into cells (11). Although Ctr3 does not possess these motifs, several cysteine residues are present throughout the protein, some of which are arranged in C*XX*C or CC potential metal binding configurations (16, 35). These motifs are found in the copper metalloregulatory transcription factors Ace1, Amt1, and Mac1, in the copper chaperone Cox17, and the metallothionein Cup1. To determine whether the cysteine residues are important for Ctr3 function, site-directed mutagenesis was used to convert each individual cysteine codon to that encoding serine. In addition, several Ctr3 tyrosine residues, which have the potential to bind Cu, were changed to phenylalanine in the same fashion. To assess the effects of these mutations on Ctr3 function, plasmids expressing the mutant proteins were transformed into a *ctr1*Δ *ctr3*Δ yeast strain. The ability of the Ctr3 derivatives to complement the respiratory deficiency and oxidative stress sensitivity of this strain was tested by growth on ethanol as sole carbon source and in the presence of glucose and the superoxide anion generator menadione, respectively. Fig. 4*A* shows a working model for the topology of Ctr3 at the plasma membrane as predicted by TopPredII analysis (36) and indicates the location of the cysteine and tyrosine residues based on this model. The results of complementation analysis, summarized in Fig. 4*B*, show that mutation of Cys-16, within the putative extracellular domain, results in a Ctr3 protein that could not complement the respiratory defect or sensitivity to menadione of the double mutant strain (Fig. 4*B, lanes 2* and *5*). Mutation of the two cysteine residues Cys-48 and Cys-51, which are arranged in a C*XX*C configuration within the first transmembrane domain, resulted in a partially functional protein that allowed very slow growth in ethanol after 5 days of incubation but failed to reverse the hypersensitivity to this concentration of menadione (Fig. 4*B, lane 7*). When the C48S,C51S mutations were combined with C199S, a cysteine residue within the third predicted transmembrane domain, the mutant protein lost residual function and failed to complement the respiratory deficiency and oxidative stress sensitivity of the double mutant (Fig. 4*B, lane 8*). In contrast, mutation of Cys-

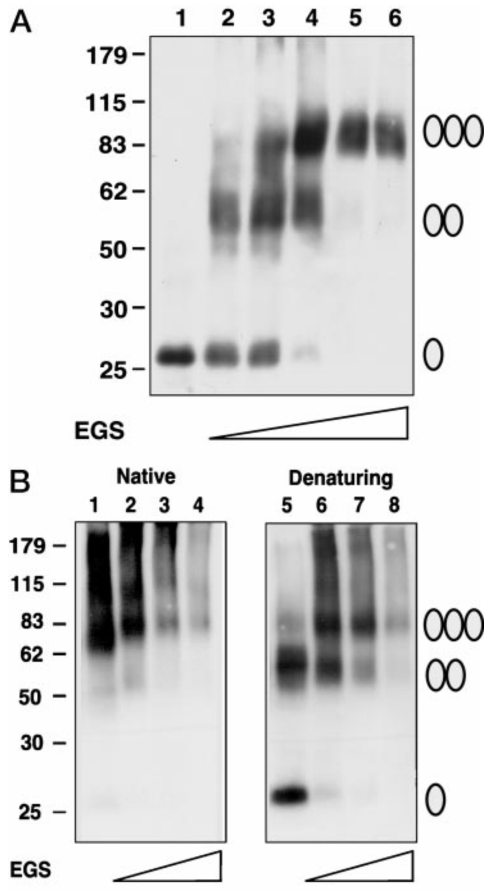

FIG. 3. **Ctr3 assembles as a trimer.** *A*, MPY17 cells (*ctr1*Δ *ctr3*Δ) were transformed with FLAG-tagged Ctr3 (pRS316-CTR3-FLAG(2)), grown to log phase, and treated with BCS for 3 h to induce Ctr3-FLAG(2) expression. *In vitro* cross-linking of Ctr3-FLAG(2) was performed using 25 μg of Triton X-100-solubilized total cell extracts using 0 (dimethyl sulfoxide solvent alone), 0.25, 0.5, 1.0, 2.0, and 3.0 mM EGS (indicated by ramp from *left* to *right*) and resolved by denaturing SDS-PAGE. Ctr3-FLAG(2) proteins were detected by immunoblotting with anti-FLAG M2 antibody. *B,* intact membranes from lysed spheroplasts prepared from MPY17 cells expressing Ctr3-FLAG(2) were grown as described above. Membranes were incubated with 0 (dimethyl sulfoxide solvent only) (*lanes 1* and *5*) or 1, 2, and 3 mM EGS (*lanes 2–4* and *6–8*) in PBS for 30 min at room temperature. The cross-linked complexes were extracted as described under "Experimental Procedures." Samples were resuspended in nondenaturing sample buffer (50% glycerol, 25 mM Tris, 0.1% bromphenol blue, 0.01 M iodoacetamide) (*Native*) or denaturing sample buffer (*Denaturing*) (same as Native buffer but including 5% β-mercaptoethanol and 2% SDS and without iodoacetamide). For both *A* and *B*, the positions of the molecular weight standards are indicated to the *left,* and on the *right*, the monomeric, dimeric, and trimeric complexes are indicated by one, two, or three *ovals*, respectively.

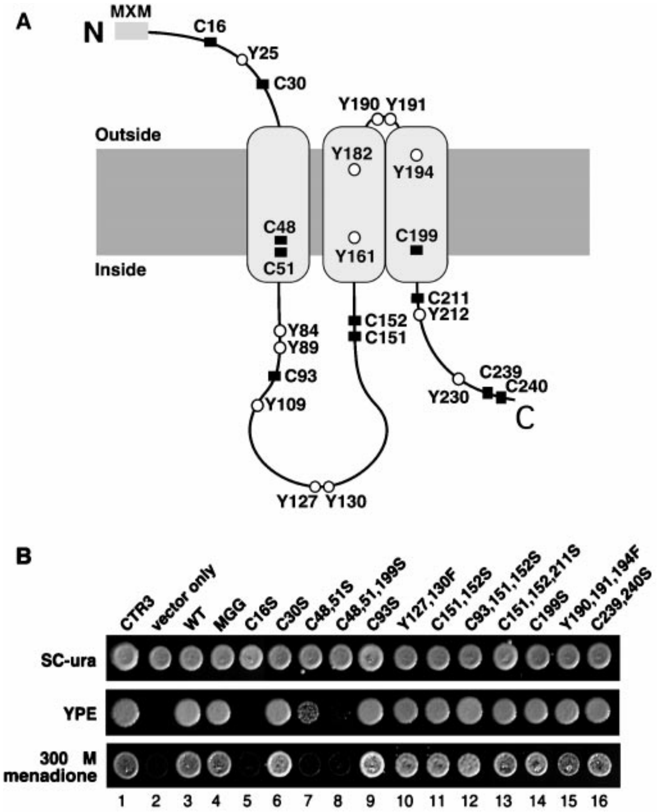

FIG. 4. **Ctr3 structure-function analysis.** *A*, topology of Ctr3 on the plasma membrane as predicted by TopPredII analysis. The location of the cysteine and tyrosine residues are indicated by a *closed square* or *open circle,* respectively. *MXM* indicates the single MXM motif on Ctr3, and *N* and *C* designate the amino and carboxyl termini of the protein, respectively. *B*, MPY17 cells transformed with wild type and mutant Ctr3 proteins were grown to log phase and spotted onto SC-ura agar, YPE agar, and SC-ura agar containing 300 μM menadione. Cells were photographed after incubation at 30 °C for 3 days on SC-ura plates and menadione plates and 5 days on YPE plates. The specific *CTR3* allele is indicated on *top*. *MGG* represents the *CTR3* allele in which the MXM domain was mutated to MSS, *WT* represents wild type SKY52 cells with a genomic copy of *CTR3*, CTR3 represents *ctr1Δ ctr3Δ* cells transformed with wild type *CTR3* on a centromeric plasmid, and vector only cells were transformed with pRS316.

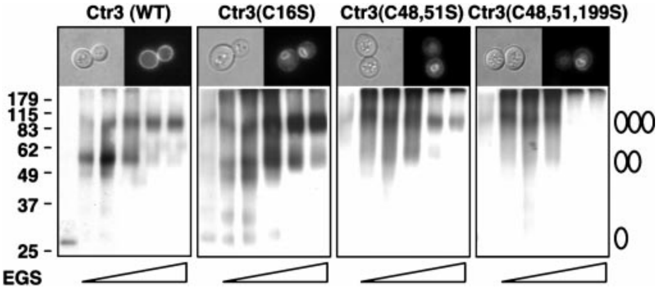

FIG. 5. **Non-functional or partially functional Ctr3 mutants are trapped in a subcellular compartment.** MPY17 cells were transformed with plasmids expressing wild type (*WT*) or mutant Ctr3-GFP fusion proteins. Cells were grown to log phase in SC-ura, and Ctr3-GFP proteins were visualized by fluorescence microscopy. The Ctr3-GFP fusions are indicated on the *top panel* with Nomarski on the *left* and the fluorescence microscope image on the *right.* The *lower panel* shows trimerization of the mutant Ctr3 proteins fused to two copies of the FLAG epitope. Molecular weights are indicated on the *left,* and monomeric, dimeric, and trimeric forms of Ctr3 and mutants are indicated by one, two, or three *ovals*, respectively, on the *right.*

199 to serine alone had no effect on Ctr3 function by these assays (Fig. 4*B, lane 14*). To ensure that the loss of function of these mutant proteins was not due to perturbation of the transmembrane environment by substituting a serine in place of a cysteine residue, the cysteines in the non-functional and partially functional mutants were mutated to alanines. The phenotypes of the cysteine to alanine mutants were indistinguishable from the cysteine to serine mutants (data not shown). Taken together, only 4 of the 11 Ctr3 cysteine residues, when mutated, have functional consequences by these analyses, Cys-16, Cys-48, Cys-51, and Cys-199.

We assessed the expression and localization of the mutant Ctr3 proteins by tagging with GFP and localization by fluorescence microscopy. The phenotypes of MPY17 cells expressing the GFP-tagged mutants with respect to growth on respiratory carbon sources were indistinguishable from the untagged mutants (data not shown). The results shown in Fig. 5 demonstrate that functional Ctr3 mutants were expressed and localized at the plasma membrane. However, the partially functional and non-functional Ctr3-GFP fusion proteins localized in a manner similar to the wild type Ctr3-GFP fusion in a *sec12-4* mutant strain at the restrictive temperature (Fig. 1*C*) suggesting that they are trapped in the ER or another portion of the secretory apparatus. *In vitro* cross-linking experiments using EGS with 1% Triton X-100-solubilized extracts from cells expressing the mutant Ctr3 proteins fused to two copies of the FLAG epitope demonstrated that these proteins can assemble to form trimers (Fig. 5). In the case of the C48S,C51S and C48S,C51S,C199S mutants, however, some high molecular weight aggregates are observed in the wells of the SDS-PAGE gels (Fig. 5). For the C48S,C51S mutant, an apparent high molecular weight multimer that is consistent with a trimer is observed in the absence of the cross-linker under denaturing conditions, and no monomer is detected suggesting that this mutant may be aggregated even though it retains residual function as assessed by its ability to confer slow growth in media containing ethanol over 5 days. The observation that these mutants can trimerize but are trapped in a secretory compartment suggests that Ctr3 assembles into a trimeric complex in this compartment. Failure of the mutant proteins to exit this compartment further suggests that at least Cys-16, Cys-48, and Cys-51 are essential for proper assembly of the complex or for interaction with other proteins that are required for exit from the ER and passage through the secretory pathway for localization at the plasma membrane.

Post-transcriptional Regulation of Ctr3—The *CTR1* and *CTR3* genes are transcriptionally regulated in response to copper or copper starvation through the interaction of the transcription factor Mac1 with copper-responsive elements in their promoters (12, 13, 37–40). In addition to transcriptional regulation, Ctr1 protein is further regulated by copper-stimulated endocytosis at copper ion concentrations from 0.1 to 10 μM, and copper stimulated degradation at the plasma membrane in the presence of copper concentrations equal to or in excess of 10 μM (14). To ascertain if Ctr3 undergoes similar forms of post-transcriptional regulation, changes in the steady state levels of Ctr3 and in Ctr3 endocytosis were examined in the absence or presence of copper and compared with Ctr1. The expression of both Ctr3-FLAG(2) and Ctr1-myc, as well as Ctr3-GFP and Ctr1-GFP, were placed under the control of the galactose-inducible glucose-repressible *GAL1-10* promoter. To assess Ctr3 steady state levels as a function of added copper, cells were grown overnight in the presence of 2% raffinose and transferred to media containing 2% raffinose and 0.5% galactose to induce the expression of Ctr3-FLAG(2) and Ctr1-myc. Transcription of the copper transporter gene was extinguished by transferring the cultures to medium containing 2% glucose, and the effects of copper on steady state protein levels were assessed after treatment with either 10 μM BCS or 10 μM copper. The results shown in Fig. 6 demonstrate that although

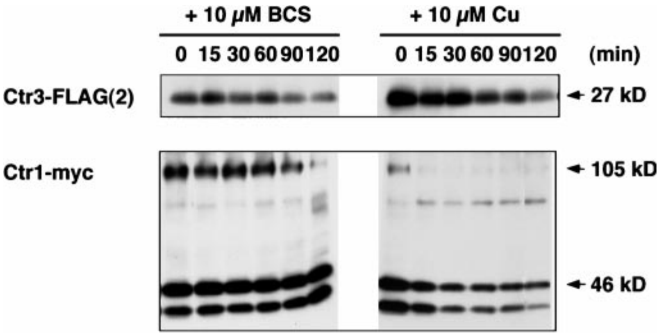

FIG. 6. **Ctr1 and Ctr3 steady state levels in response to elevated copper concentrations.** *S. cerevisiae* (W303) cells transformed with p423-Gal1-*CTR3-FLAG(2)* or p426-Gal1-*CTR1-myc* were grown as described under "Experimental Procedures." After glucose shut-off of Ctr3-FLAG(2) and Ctr1-myc expression, cells were treated with 10 μM BCS or 10 μM copper sulfate. Samples were taken at the indicated time points, and 50 μg of Triton X-100-solubilized total cell extracts were analyzed by immunoblotting. Ctr3-FLAG(2) was detected using anti-FLAG M2 antibody, and Ctr1-myc was detected with anti-c-*myc* 9E10 antibody. The *arrow* on the *right* indicates the molecular mass of Ctr3 (27 kDa) and Ctr1-myc (105 and 46 kDa).

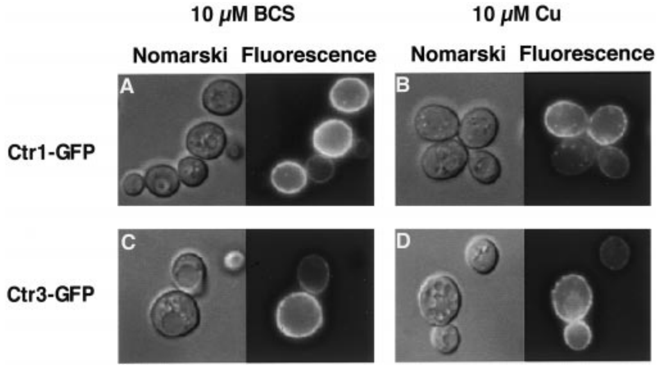

FIG. 7. **Ctr1 but not Ctr3 undergoes copper-stimulated endocytosis.** *S. cerevisiae* wild type (RH1800) cells were transformed with p426-Gal1-*CTR3-GFP* and p426-Gal1-*CTR1-GFP*, grown, and harvested as described under "Experimental Procedures." Cells were incubated at 15 °C for 15 min and then treated with 10 μM BCS (*A* and *C*) or 10 μM copper (*B* and *D*) for 60 min at 15 °C. Ctr1-GFP and Ctr3-GFP were visualized by fluorescence microscopy and photographed as described under "Experimental Procedures."

Ctr1 degradation is stimulated in a time-dependent manner in the presence of 10 μM copper, the same copper concentration has little if any effect on the stability the Ctr3 as compared with the control culture. In several experiments, we observed the same rate of decrease in the steady state levels of Ctr3 in the presence of 10 μM BCS or copper. Thus, as shown in Fig. 6 (*top panel*), treatment of cells with 10 μM copper does not affect the stability of Ctr3. In other experiments, the immunoblots were stripped and analyzed with antibodies against phosphoglycerate kinase to ensure equal loading of protein extracts in all lanes (data not shown). Under these conditions Ctr3 is rather stable, with a half-life of about 90 min in the presence or absence of added copper. On the other hand, Ctr1 has a half-life of approximately 90 min in the presence of 10 μM BCS and less than 15 min in the presence of 10 μM copper. Thus, as shown here and as previously shown (14), whereas Ctr1 undergoes copper-dependent degradation, Ctr3 steady state levels are not altered when yeast cells are subjected to the same copper treatment.

To ascertain whether, like Ctr1 (14), Ctr3 endocytosis is stimulated by elevated copper levels, cells transformed with plasmids expressing the Ctr3-GFP or Ctr1-GFP fusion proteins from the *GAL1-10* promoter were examined by fluorescence microscopy. The results shown in Fig. 7 demonstrate that, as previously shown using a Ctr1-myc protein (14), Ctr1-GFP undergoes enhanced endocytosis in the presence of copper as indicated by the presence of presumptive endocytic vesicles that appear in a time-dependent manner after copper addition but not in BCS-treated control cultures. Under these same conditions, endocytosis of Ctr3-GFP from the plasma membrane is not stimulated. As a control, both plasmids were also transformed into *S. cerevisiae end3-1* mutants (25) that are blocked for endocytosis. In this strain, neither Ctr1-GFP nor Ctr3-GFP undergoes endocytosis in the presence or absence of copper (data not shown). Taken together these results demonstrate that whereas the genes encoding Ctr1 and Ctr3 are similarly regulated in a copper-dependent manner at the transcriptional level, at the post-transcriptional level the Ctr1 and Ctr3 proteins are regulated in a distinct manner.

DISCUSSION

Our studies on the Ctr3 high affinity copper transport protein represent the initial characterization of its localization, assembly, structure-function analysis, and post-transcriptional regulation. By using a functional Ctr3-GFP fusion protein, we firmly establish that, consistent with its role in copper uptake, Ctr3 is localized to the yeast plasma membrane. Like most plasma membrane proteins, Ctr3 traverses the secretory pathway for proper localization. Whereas most *S. cerevisiae* permeases and transport proteins possess 6–12 transmembrane domains (30), the copper transport family of proteins identified thus far possess only 3 such domains. To begin to understand the mechanism by which these proteins deliver copper into the cell, we carried out experiments to determine how the Ctr3 protein assembles as a functional copper transporting permease. By using co-immunoprecipitation experiments, we show that Ctr3 self-assembles to form a specific homo-multimeric complex. Through *in vitro* cross-linking with EGS using Triton X-100-solubilized total cell extracts and cross-linking of intact membranes, we show that assembly of the Ctr3 complex is consistent with a trimer. Nine transmembrane domains from three Ctr3 molecules could form a pore through which copper can be translocated into the cell. Although we have not assessed if Ctr1 and Ctr3 can form mixed multimers, this is clearly not obligatory for their function in high affinity copper transport since both proteins can function efficiently independent of the other.

How does Ctr3 interact with copper to deliver copper into the cell? The established or putative copper transporters in yeast, Ctr1 and Ctr4, hCtr1, and mCtr1 possess a conserved sequence, MX_2MXM, in the predicted extracellular domain that is proposed to interact with copper or copper bound to another ligand in the environment (15). This motif, however, is lacking in Ctr3. Instead, Ctr3 has 11 cysteine residues throughout the protein that may be involved in copper binding. We assessed the potential role of these residues on Ctr3 function and biogenesis by mutating the cysteines to serines or alanines. Of these mutations, only Cys-16, Cys-48, and Cys-51 resulted in a non-functional or partially functional Ctr3 protein as assessed by the ability of these proteins to complement the respiratory deficiency and oxidative stress sensitivity of a *ctr1*Δ *ctr3*Δ mutant strain. By *in vitro* cross-linking, we show that these mutants are capable of trimerization, with the C48S,C51S and C48S,C51S,C199S mutants forming higher molecular weight aggregates. Through fluorescence microscopy on the GFP-tagged mutants, we found that these mutants fail to exit an intracellular compartment likely to be the ER. Although our results preclude us from addressing the role of these residues in copper uptake at the plasma membrane, they suggest that these cysteine residues may be important for the assembly of the Ctr3 complex in the secretory pathway. Since proper assembly and folding of newly synthesized proteins begins in the ER (41), it is possible that these residues may be important for interacting with proteins such as phosphodisulfide isomerases that catalyze the formation of appropriate disulfide bonds (42) and other chaperones that may be required for proper folding and assembly of Ctr3 for passage through the secretory pathway. Furthermore, these results also suggest that the assembly of the Ctr3 complex takes place as the protein traverses the secretory pathway.

Because copper is essential and toxic, yeast genes encoding high affinity copper transporters are tightly regulated at the transcriptional level by copper-sensing transcription factors (12, 13, 17, 37, 43). Furthermore, *S. cerevisiae* Ctr1 is regulated at the post-transcriptional level through endocytosis at low copper concentrations and degradation at the plasma membrane in the presence of elevated copper concentrations (14). Since Ctr1 and Ctr3 are functionally redundant, we compared their degradation and endocytosis in response to elevated copper concentrations. Surprisingly, the post-transcriptional regulation of Ctr3 is distinct from Ctr1. Whereas Ctr1 is degraded rapidly in the presence of 10 μM copper, the stability of Ctr3 is not affected by increased copper concentration in the media. Furthermore, whereas Ctr1 undergoes enhanced endocytosis in the presence of 10 μM copper, under the same conditions Ctr3 protein is observed to remain at the plasma membrane. Thus, although both proteins may undergo constitutive endocytosis under copper-replete conditions, endocytosis of Ctr1, but not Ctr3, is stimulated in response to copper. Therefore, whereas transcription of the genes encoding both Ctr1 and Ctr3 is regulated similarly in response to copper, the Ctr1 and Ctr3 proteins are regulated differentially by copper. These observations provide the first distinction between these two high affinity copper transport proteins that may be a consequence of the differences between their structures.

The *S. pombe* Ctr4 and putative mammalian high affinity copper transporters appear to be a combination of Ctr1 and Ctr3 (15). Most of these proteins possess the Mets domain present in Ctr1, but not Ctr3, in their predicted extracellular domains and have a high homology to the transmembrane domains of Ctr3. The conservation of these domains among these transporters suggests that they may be important for the proper assembly, function, and regulation of these proteins. Understanding the mechanisms for copper-stimulated post-transcriptional regulation of Ctr1 will be an important step for elucidating another mechanism by which organisms modulate the accumulation of copper. Identifying the amino acid residues in Ctr1 that are required for this process and their conservation in other eukaryotic copper transporters will provide insights into how these organisms regulate intracellular copper levels. Furthermore, structure-function analyses to identify the residues that are important for the function and assembly of the copper transporters will provide insights into the mechanism by which these proteins can translocate copper into the cell. Since Ctr3 is a module that is present in all copper transporters, it provides an important tool for dissecting the pathways that govern this regulatory mechanism and the assembly of these proteins.

Acknowledgments—We are grateful to Drs. Robert Fuller, Kevin Morano, and Jason Brickner and members of the Thiele and Fuller laboratories for helpful discussions. We thank Jaekwon Lee and Hao Zhou for critical reading of the manuscript. We thank Jeanne Hirsch, Andy Dancis, Howard Riezman, and Bob Fuller for strains and plasmids used in this study and Amy Chang and T. Doering for antibodies against Pma1 and Gas1. We also thank Chen Kuang and Bisan Salhi for technical assistance.

REFERENCES

1. Linder, M. C. (1991) *Biochemistry of Copper* (Frieden, E., ed) Vol. 10, Plenum Publishing Corp., New York
2. Halliwell, B., and Gutteridge, J. M. C. (1984) *Biochem. J.* **219,** 1–4
3. Hassett, R., and Kosman, D. J. (1995) *J. Biol. Chem.* **270,** 128–134
4. Georgatsou, E., Mavrogiannis, L. A., Fragiadakis, G. S., and Alexandraki, D. (1997) *J. Biol. Chem.* **272,** 13786–13792
5. Dancis, A., Yuan, D. S., Haile, D., Askwith, C., Eide, D., Moehle, C., Kaplan, J., and Klausner, R. D. (1994) *Cell* **76,** 393–402
6. Knight, S. A., Labbe, S., Kwon, L. F., Kosman, D. J., and Thiele, D. J. (1996) *Genes Dev.* **10,** 1917–1929
7. Lin, S. J., Pufahl, R. A., Dancis, A., O'Halloran, T. V., and Culotta, V. C. (1997) *J. Biol. Chem.* **272,** 9215–9220
8. Pufahl, R. A., Singer, C. P., Peariso, K. L., Lin, S. J., Schmidt, P. J., Fahrni, C. J., Culotta, V. C., Penner-Hahn, J. E., and O'Halloran, T. V. (1997) *Science* **278,** 853–856
9. Glerum, D. M., Shtanko, A., and Tzagoloff, A. (1996) *J. Biol. Chem.* **271,** 14504–14509
10. Culotta, V. C., Klomp, L. W., Strain, J., Casareno, R. L., Krems, B., and Gitlin, J. D. (1997) *J. Biol. Chem.* **272,** 23469–23472
11. Dancis, A., Haile, D., Yuan, D. S., and Klausner, R. D. (1994) *J. Biol. Chem.* **269,** 25660–25667
12. Labbe, S., Zhu, Z., and Thiele, D. J. (1997) *J. Biol. Chem.* **272,** 15951–15958
13. Yamaguchi-Iwai, Y., Serpe, M., Haile, D., Yang, W., Kosman, D. J., Klausner, R. D., and Dancis, A. (1997) *J. Biol. Chem.* **272,** 17711–17718
14. Ooi, C. E., Rabinovich, E., Dancis, A., Bonifacino, J. S., and Klausner, R. D. (1996) *EMBO J.* **15,** 3515–3523
15. Labbe, S., and Thiele, D. J. (1999) *Trends Microbiol.* **7,** 500–505
16. Koch, K. A., Pena, M. M., and Thiele, D. J. (1997) *Chem. Biol.* **4,** 549–560
17. Labbe, S., Pena, M. M., Fernandes, A. R., and Thiele, D. J. (1999) *J. Biol. Chem.* **274,** 36252–36260
18. Inouye, S., and Tsuji, F. I. (1994) *FEBS Lett.* **341,** 277–280
19. Knappik, A., and Pluckthun, A. (1994) *BioTechniques* **17,** 754–761
20. Evan, G. I., Lewis, G. K., Ramsay, G., and Bishop, J. M. (1985) *Mol. Cell. Biol.* **5,** 3610–3616
21. Mumberg, D., Muller, R., and Funk, M. (1994) *Nucleic Acids Res.* **22,** 5767–5768
22. Ausubel, F. M., Brent, R., Kingston, R. E., Moore, D. D., Seidman, J. G., Smith, J. A., and Struhl, K. (eds) (1987) *Current Protocols in Molecular Biology*, John Wiley & Sons, Inc., New York
23. Belden, W. J., and Barlowe, C. (1996) *J. Biol. Chem.* **271,** 26939–26946
24. Marcusson, E. G., Horazdovsky, B. F., Cereghino, J. L., Gharakhanian, E., and Emr, S. D. (1994) *Cell* **77,** 579–586
25. Raths, S., Rohrer, J., Crausaz, F., and Riezman, H. (1993) *J. Cell Biol.* **120,** 55–65
26. Urbanowski, J. L., and Piper, R. C. (1999) *J. Biol. Chem.* **274,** 38061–38070
27. Liu, X. D., Liu, P. C., Santoro, N., and Thiele, D. J. (1997) *EMBO J.* **16,** 6466–6477
28. Nakano, A., Brada, D., and Schekman, R. (1988) *J. Cell Biol.* **107,** 851–863
29. Kaiser, C. A., and Schekman, R. (1990) *Cell* **61,** 723–733
30. Serrano, R. (1991) in *Molecular Biology of the Yeast Saccharomyces* (Broach, J. R., Pringle, J., and Jones, E. W., eds) Vol. 1, pp. 523–585, Cold Spring Harbor Laboratory, Cold Spring Harbor, NY
31. Rolfs, A., and Hediger, M. A. (1999) *J. Physiol.* (*Lond.*) **518,** 1–12
32. Wang, Q., and Chang, A. (1999) *EMBO J.* **18,** 5972–5982
33. Fankhauser, C., and Conzelmann, A. (1991) *Eur. J. Biochem.* **195,** 439–448
34. Abdella, P. M., Smith, P. K., and Royer, G. P. (1979) *Biochem. Cell Biol.* **87,** 734–742
35. Winge, D. R. (1998) *Prog. Nucleic Acids Res. Mol. Biol.* **58,** 165–195
36. Claros, M. G., and von Heijne, G. (1994) *Comput. Appl. Biosci.* **10,** 685–686
37. Jensen, L. T., and Winge, D. R. (1998) *EMBO J.* **17,** 5400–5408
38. Jensen, L. T., Posewitz, M. C., Srinivasan, C., and Winge, D. R. (1998) *J. Biol. Chem.* **273,** 23805–23811
39. Joshi, A., Serpe, M., and Kosman, D. J. (1999) *J. Biol. Chem.* **274,** 218–226
40. Georgatsou, E., and Alexandraki, D. (1999) *Yeast* **15,** 573–584
41. Hammond, C., and Helenius, A. (1995) *Curr. Opin. Cell Biol.* **7,** 523–529
42. Gilbert, H. F. (1997) *J. Biol. Chem.* **272,** 29399–29402
43. Jungmann, J., Reins, H. A., Lee, J., Romeo, A., Hassett, R., Kosman, D., and Jentsch, S. (1993) *EMBO J.* **12,** 5051–5056
44. Pena, M. M., Koch, K. A., and Thiele, D. J. (1998) *Mol. Cell. Biol.* **18,** 2514–2523